JOURNAL OF CATALYSIS 87, 325–331 (1984)

Catalytic Hydrodeoxygenation of Benzofuran and *o*-Ethylphenol

CHUNG-LI LEE AND DAVID F. OLLIS[1]

Department of Chemical Engineering, University of California, Davis, California 95616

Received December 7, 1982; revised December 22, 1983

The catalytic hydrodeoxygenations (HDO) of benzofuran and of a related compound, *o*-ethylphenol, are examined on a presulfided CoMo/γAl_2O_3 catalyst. The benzofuran reaction proceeds with hydrogenation of the oxygen-containing ring as the first step; two sequential reaction intermediates, 2,3-dihydrobenzofuran and *o*-ethylphenol, were identified. The major HDO products included ethylbenzene, ethylcyclohexane, and ethylcyclohexene. A mechanism for the hydrodeoxygenation of benzofuran is proposed, requiring hydrogenation to *o*-ethylphenol prior to hydrodeoxygenation. The apparent reaction rate constants and activation energies for all conversions of benzofuran or *o*-ethylphenol are evaluated for the rate equations of Langmuir–Hinshelwood type.

INTRODUCTION

The presence of sulfur, nitrogen, and oxygen in various molecular structures is found in coal-derived products, shale oil, tar sand, and petroleum. An extensive literature in catalytic hydrotreating processes has been developed from examination of hydrodesulfurization and hydrodenitrogenation. The removal of sulfur and nitrogen is effected both to remove potential poisons for downstream refinery catalysts and to render resultant fuel products environmentally acceptable. The removal of oxygen occurs simultaneously with HDS and HDN; thus an unavoidable additional hydrogen consumption price must be paid. Further, if HDO (hydrodeoxygenation) inhibits HDS and/or HDN, then the presence of oxygenates in HDS and/or HDN feedstocks may exact further processing penalties in the form of slower net rates of reaction.

Model-compounds studies on sulfur removal from benzothiophene (*1–3*), dibenzothiophene (*3–7*), and thianthrene (*7*) are reported in the literature. Studies on nitrogen removal include pyridine (*8, 9*), pyrrole (*11*), indole (*10, 11*), quinoline (*12*), and acridine (*12*). The conversion of mixtures of model compounds is demonstrated by Rollman (*13*), Badilla-Ohlham (*14*), and Satterfield (*15*). The report from Satterfield clearly illustrates the interactions between hydrodesulfurization of thiophene and hydrodenitrogenation of pyridine. However, the hydrodeoxygenation of oxygen-containing compounds is poorly understood at the present time. Three early works are reported on the reduction of phenolic compounds (*16*), benzofuran and dibenzofuran (*17, 18*). Very recently Shah has examined the kinetics and reaction network of dibenzofuran HDO (*19*) in detail. The catalytic hydrodeoxygenation of cresols, and their role in interactions of HDO/HDN and HDO/HDS were elucidated in this laboratory by Odebunmi (*20*). We examine in this paper the hydrodeoxygenation pathways of benzofuran and its major reaction intermediate, *o*-ethylphenol. The corresponding interactions in simultaneous HDO/HDS are reported in a companion paper.

EXPERIMENTAL DETAILS

Equipment

Experiments were carried out in a continuous trickle reactor with a high-pressure liquid pump (ISCO Model 314, 2850-psi metering pump). The gas flow was measured by a thermal mass flow meter (Brooks In-

---

[1] Current address: Department of Chemical Engineering, Box 5035, North Carolina State University, Raleigh, N.C. 27650.

0021-9517/84 $3.00

strument Division Model DS-5810). The pressure was indicated by a digital system (Autoclave Engineers Model No. DPA-0022) and controlled by a Bourdon gauge. A digital temperature indicator (Omega Engineering Inc. Model 400A) with two thermocouple probes (Omega Engineering Inc. Chromel–Constantan Type E) was used to measure the temperature inside and outside the reactor.

Catalyst

The catalyst $CoO–MoO_3/\gamma Al_2O_3$ (American Cyanamid Aero HDS-2A, composition (MoO_3, 15.4%; CoO, 3.2%, Na_2O, 0.03%; Fe, 0.03%; SO_4, 0.3%; SiO_2, 0.1%), 310 m^2/g, pore volume = 0.75 cc/g) was crushed and sieved to 40 mesh and sulfided prior to use. The sulfiding or the regeneration of the catalyst included 17 hr of reduction (400°C) with pure hydrogen, and 3 hr of sulfiding in 10% H_2S/H_2 flowing mixture at 400°C; subsequently, the catalyst was cooled to the desired temperature under pure argon.

Chemicals

All gases were supplied by Matheson in high purity. Chemicals used in this experiment were from Aldrich Chemical Company and used without further purification.

Procedure and Analysis

N-Heptylmercaptan was added in every feedstream in a concentration of 0.0075 *M* to maintain the sulfided form of the catalyst. The feed concentration of benzofuran or *o*-ethylphenol was 0.15 *M*. Variation of liquid flow rate from 13 to 3 cc/hr changed the space velocity for study at fixed temperatures. The catalyst was regenerated after a set of experiments were completed. Liquid samples were analyzed on a Sigma 1 Perkin–Elmer gas chromatograph; component identifications were established on a Finnigan GC/MS. The hydrogen pressure was 69 atm unless noted otherwise.

Kinetic Analysis and Results

Singhal *et al.* (*7*) have revealed that a Langmuir–Hinshelwood kinetic model fits the kinetics of hydrodesulfurization of dibenzothiophene on sulfided $CoO–MoO_3/\gamma Al_2O_3$ catalyst. Their model assumed two sites, with competitive adsorption of reactant and H_2S on one site, and a noncompetitive adsorption of H_2 on the other. Similar kinetic forms are applicable to HDO reactions involving cresols (Odebunmi (*20*)). In the present paper, we consider a corresponding Langmuir–Hinshelwood kinetic model with two active sites for hydrodeoxygenation of benzofuran and *o*-ethylphenol. We may write a differential rate expression for competitive adsorption of reactant, oxygenated intermediates (C_{P1}, C_{P2}, etc.), water (C_w), and trace mercaptan (C_S) on one site, and adsorption of hydrogen on the other site, as

$$F\,dX_{HDO} = \frac{k_{HDO}K_R C_R f(P_{H_2})}{1 + K_R C_R + K_w C_w + \Sigma(K_{Pi}C_{Pi}) + K_S C_S}\,dw. \quad (1)$$

The actual kinetic behavior of the system is, we show later, nearly first order. The finding of Singhal *et al.* (*7*) that H_2S and dibenzothiophene binding are of nearly identical strength encourages the notion that water and oxygenates bind with similar strength. Thus we may simplify Eq. (1) by assuming that $K_{Pi} \sim K_w$ (all *i*). Then since $[C_w + \Sigma(C_{Pi}) + C_R] = C_R^0$, Eq. (1) would become

$$F\,dX_{HDO} = \frac{(k_{HDO}K_R)C_R}{1 + K_R C_R^0 + K_S C_S} f(H_2)\,dw.$$

Under our operating conditions, the trace mercaptan is ~100% converted, and hydrogen pressure is constant throughout the bed, i.e., neither C_S nor $f(H_2)$ are dependent on position in the bed or flow rate. For such a situation, the above equation is first order, giving Eq. (2) on integration:

$$-\ln(1 - X_{HDO}) = kC_R^0(w/F) = k(w/Q), \quad (2)$$

where

$$k = \frac{k_{\mathrm{HDO}} \cdot K_{\mathrm{R}}}{(1 + K_{\mathrm{R}}C_{\mathrm{R}}^{0} + K_{\mathrm{S}}C_{\mathrm{S}})} \cdot f(\mathrm{H_2}),$$

$$Q = F/C_{\mathrm{R}}^{0},$$

and

$$X_{\mathrm{HDO}} = \Sigma \frac{\text{hydrodeoxygenated products}}{\text{feed benzofuran}}.$$

Similarly, the rate equation for the hydrogenation of benzofuran to 2,3-dihydrobenzofuran and *o*-ethylphenol could be written as follows under the assumption that the equilibrium adsorption coefficient for benzofuran (K_{R}), 2,3-dihydrobenzofuran (K_{P1}), and *o*-ethylphenol (K_{P2}) are all approximately the same:

$$-\ln(1 - X_{\mathrm{H}}) = k'(w/F), \tag{3}$$

where

$$k' = \frac{k_{\mathrm{Hyd}}K_{\mathrm{R}}C_{\mathrm{R}}^{0}K_{\mathrm{H_2}}P_{\mathrm{H_2}}}{(1 + K_{\mathrm{R}}C_{\mathrm{R}}^{0} + K_{\mathrm{S}}C_{\mathrm{S}})(1 + K_{\mathrm{H_2}}P_{\mathrm{H_2}})}$$

and

$$X_{\mathrm{H}} = \Sigma \frac{\text{hydrogenated products}}{\text{feed benzofuran}}.$$

In the following section, we present experimental results which indicate nearly first-order conversions for both HDO and hydrogenation of benzofuran, one of the major heterocyclic compounds found in coal liquids (*21*, *22*).

Hydrogenation of Benzofuran

Below 260°C, 2,3-dihydrobenzofuran and *o*-ethylphenol are the only products detected, with no deoxygenated products observed. Figure 1 shows the hydrogenation conversion of benzofuran versus (space velocity)$^{-1}$ at 220, 240, and 260°C. The 2,3-dihydrobenzofuran appears before appreciable formation of *o*-ethylphenol; this behavior is especially clear at 220°C. Thus, hydrogenation of the $C_2{=}C_3$ double bond in compound **1** (benzofuran) occurs and then the hydrogenolysis of C_3—O bond to give *o*-ethylphenol:

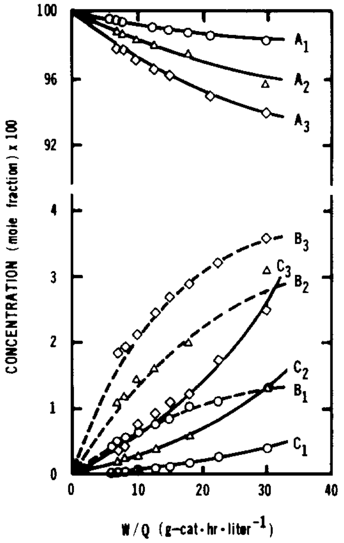

FIG. 1. Mole fraction vs the reciprocal of space velocity in hydrogenation of benzofuran: (A) unreacted benzofuran; (B) 2,3-dihydrobenzofuran; (C) *o*-ethylphenol. Subscripts 1, 2, and 3 indicate temperatures of 220, 240, and 260°C, respectively.

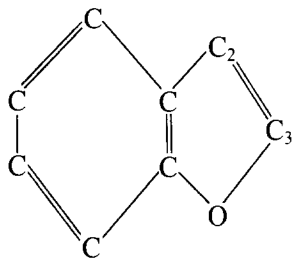

Benzofuran

1

These results follow the consecutive reaction network

$$\begin{tikzcd} \text{benzofuran} \arrow[r, "H_2", "\text{catalyst}"'] & \text{2,3-dihydrobenzofuran} \arrow[d, "H_2,\ \text{catalyst}"] \\ & o\text{-ethylphenol} \end{tikzcd} \tag{4}$$

ruling out the possibility of direct extrusion of oxygen from benzofuran. In apparent contrast, the direct extrusion of oxygen and sulfur from *di*benzofuran and *di*benzothiophene was noted by the early appearance of biphenyl in the products (*19*, *4*).

For these hydrogenations of benzofuran,

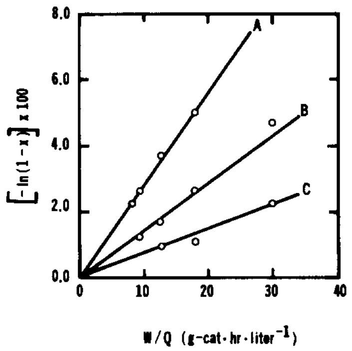

FIG. 2. Plot of $-\ln(1 - X)$ vs w/Q for the hydrogenation of benzofuran under 1022 psi of H_2: (A) 260°C; (B) 240°C; (C) 220°C.

the essentially linear relationship of $-\ln(1 - X_H)$ vs reciprocal space velocity is shown in Fig. 2. The apparent first-order rate constants calculated from these slopes are used to construct the corresponding Arrhenius plot (Fig. 3), giving $E_a = 19.4$ kcal/mol and $A = 2.14 \times 10^5$ liters hr^{-1} (g-cat)$^{-1}$.

Hydrodeoxygenation of Benzofuran

As the temperature was increased above 260°C, the mole fraction of *o*-ethylphenol in the exit products became larger than that of the 2,3-dihydrobenzofuran, as would be suggested also by the data in Fig. 1.

Appreciable amounts of deoxygenated products were detected as the temperature was raised above 310°C. The major deoxygenated products were ethylbenzene, ethylcyclohexene, and ethylcyclohexane. Trace amounts of cyclohexene and cyclohexane were noted, evidently formed from further hydrogenolysis of ethylcyclohexene and ethylcyclohexane.

The hydrodeoxygenation conversion X_{HDO} of benzofuran was calculated as the sum of all deoxygenated products (ethylbenzene, ethylcyclohexene, ethylcyclohexane, cyclohexene, and cyclohexane) divided by the initial benzofuran concentration. A plot of $\ln(1 - X_{HDO})$ vs reciprocal space velocity (Fig. 4) shows linear behavior for $T = 310$–345°C and differential conversions to ~4.5%. The apparent first-order rate constants were used for the Arrhenius plot in Fig. 3, giving $E_a = 33$ kcal/mol and $A = 2.1 \times 10^9$ liters hr^{-1} (g-cat)$^{-1}$.

Evaluation of the benzofuran equilibrium adsorption coefficient K_R and intrinsic HDO rate constant k_{HDO} was attempted from the k values calculated from Eq. (2) from Figs. 5 and 6. Plots of $1/k$ vs benzofuran concentration (C_R^0) (Fig. 7) appear to be represented by straight lines. From the above definition for k (equation following Eq. (2)),

$$\text{intercept} = \frac{(1 + K_S C_S)}{k_{HDO} K_R f(H_2)},$$

$$\text{slope} = \frac{1}{k_{HDO} f(H_2)}.$$

The slope results give values for $k_{HDO} f(H_2)$ at 310 and 325°C of 1.6×10^{-4} mole hr^{-1} (g-

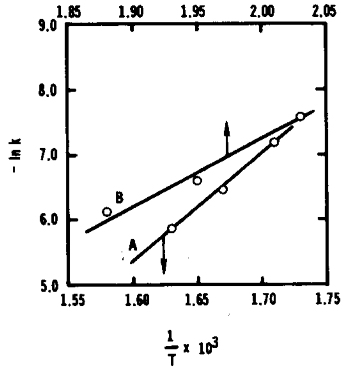

FIG. 3. Arrhenius plots of $-\ln k$ vs $1/T \times 10^3$: (A) hydrodeoxygenation of benzofuran; (B) hydrogenation of benzofuran.

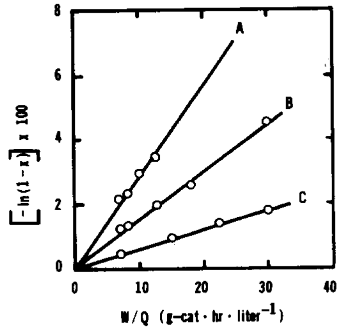

FIG. 4. Plot of $-\ln(1 - X)$ vs w/Q for the hydrodeoxygenation of benzofuran: (A) 340°C; (B) 325°C; (C) 310°C ($C_R^0 = 0.15$ *M*).

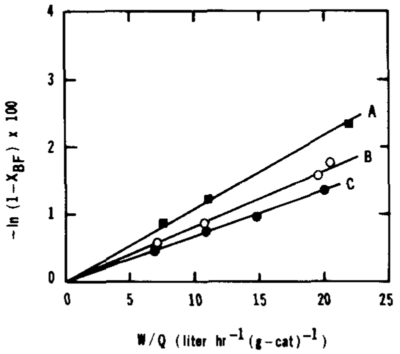

FIG. 5. Plot of $-\ln(1 - X_{BF})$ vs w/Q for hydrodeoxygenation of benzofuran at 310°C: (A) 0.15 *M* BF; (B) 0.20 *M* BF; (C) 0.25 *M* BF.

cat)$^{-1}$ and 3.5×10^{-4} mole hr^{-1} (g-cat)$^{-1}$, respectively. The essentially zero value of the intercept indicates that K_R is large, i.e., $K_R > 30$ liters/mole at each temperature.

Hydrodeoxygenation of o-Ethylphenol

o-Ethylphenol appeared from Eq. (1) to be the reaction intermediate prior to the deoxygenation. To clarify the HDO of benzofuran, we studied the HDO of *o*-ethylphenol as a single component feed. The result shows the same deoxygenated product distribution as benzofuran does, although the reaction occurs at much lower temperatures than for benzofuran. The linearity of $-\ln(1 - X_{HDO})$ vs reciprocal of space velocity, and of the Arrhenius plot, are shown in Figs. 8 and 9, respectively. The apparent activation energy ($E_a = 16.8$ kcal/mol) is considerably smaller than that for benzofuran hydrodeoxygenation.

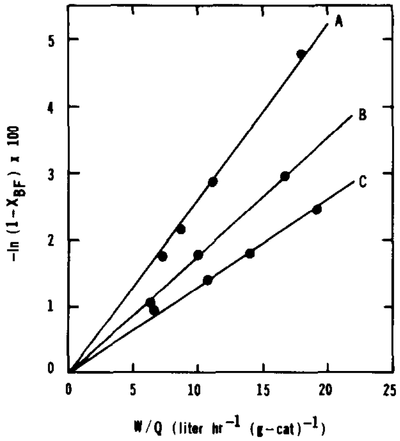

FIG. 6. Plot of $-\ln(- X_{BF})$ vs w/Q for hydrodeoxygenation of benzofuran at 325°C: (A) 0.15 *M* BF; (B) 0.20 *M* BF; (C) 0.25 *M* BF.

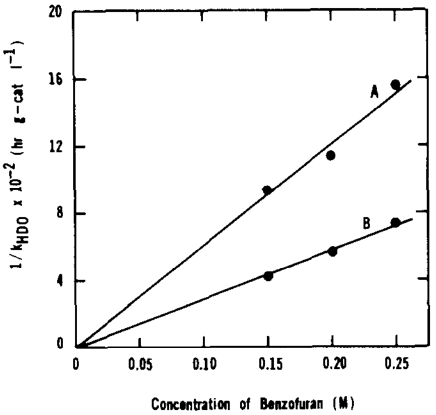

FIG. 7. Plot of $1/k'_{HDO}$ vs BF concentration for the hydrodeoxygenation of benzofuran: (A) 310°C; (B) 325°C.

Throughout this experiment, neither benzofuran nor 2,3-dihydrobenzofuran was detected. This result simply indicates that "dehydrocyclization" is not feasible for *o*-ethylphenol on this catalyst. The irreversibility of the hydrogenolysis of 2,3-dihydrobenzofuran to *o*-ethylphenol could be understood by this evidence.

Dependence of Hydrogen

Determination of the role played by hydrogen was examined at 325°C at fixed liq-

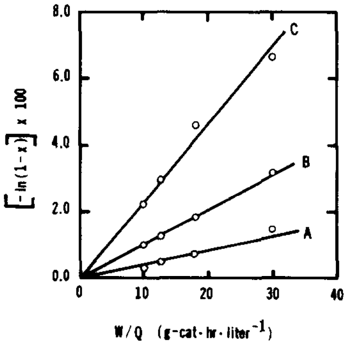

FIG. 8. Plot of $-\ln(1 - X)$ vs w/Q for the hydrodeoxygenation of *o*-ethylphenol: (A) 220°C; (B) 240°C; (C) 260°C, under 1022 psi of H_2.

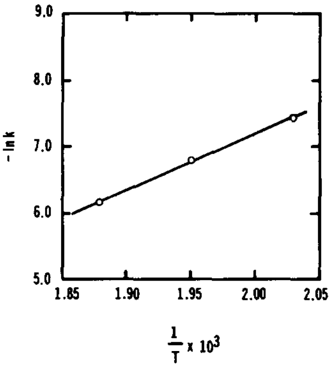

FIG. 9. Arrhenius plot of $-\ln k$ vs $1/T \times 10^3$ for the hydrodeoxygenation of *o*-ethylphenol under 1022 psi of H_2.

uid flow rate with various hydrogen pressures. Figure 10 indicates a gradual approach to surface saturation, giving a hydrogen binding constant K_{H_2} (≡ inverse of Fig. 10 slope) of 0.01 atm^{-1}.

Reaction Pathway

Our experimental results show that

(i) the *hydrogenation* reactions for benzofuran conversion to 2,3-dihydrobenzofuran and then *o*-ethylphenol occur appreciably at 200°C;

(ii) the *hydrodeoxygenation* of benzofuran and of *o*-ethylphenol produces the same deoxygenated products, yet no 2,3-dihydrobenzofuran or benzofuran is formed from *o*-ethylphenol;

(iii) the *hydrodeoxygenation* of an *o*-ethylphenol feed occurs nearly 100°C lower than hydrodeoxygenation of a benzofuran feed.

These results appear to be best rationalized by the reaction network proposed in Fig. 11. The hydrogenative conversions of benzofuran to *o*-ethylphenol occur first. The product distribution obtained from *o*-ethylphenol deoxygenation, without formation of any 2,3-dibenzofuran, establishes the obligatory sequential passage of all benzofuran through the ethylphenol prior to deoxygenation. The final dealkylations appear to occur to only small extents on our catalysts.

The considerable ease of *o*-ethylphenol HDO at 220–260°C in the absence of benzofuran indicates that benzofuran (and/or 2,3-dihydrobenzofuran) binds considerably more strongly to the catalyst than does *o*-ethylphenol, thus completely inhibiting HDO of the latter at temperatures below 300°C. This inhibition interpretation is supported by the very considerable difference in apparent activation energies for HDO of benzofuran (E_a = 33 kcal/mole) vs *o*-ethylphenol (E_a = 17 kcal/mole). As both HDO sequences move through the same slow

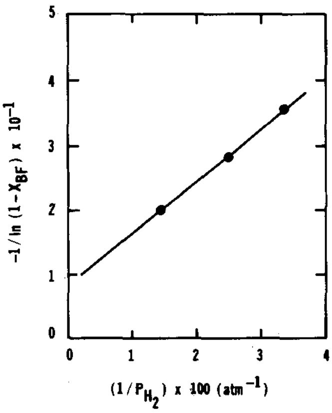

FIG. 10. Plot of $-\ln(1 - X_{BF})$ vs (hydrogen pressure)$^{-1}$ at fixed liquid flow rate 5 cc/hr and fixed benzofuran concentration at 325°C.

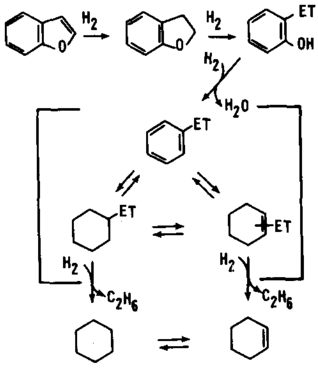

FIG. 11. Reaction network (proposed) for the hydrodeoxygenation of benzofuran (order of appearance of ethylbenzene vs ethylcyclohexane vs ethylcyclohexene unknown).

step of *o*-ethylphenol HDO, a higher apparent activation energy under the differential conversion conditions of the present study must be due to the thermodynamics of strong binding by benzofuran or 2,3-dihydrobenzofuran. Thus, our original assumption concerning binding strengths (leading to Eqs. (2) and (3)) should be modified to read

$$(K_{\text{benzofuran}},\ K_{2,3\text{-dibenzofuran}}) \gg K_{o\text{-ethylphenol}}.$$

As a final comment, the modest curvature for the benzofuran concentration vs reciprocal space velocity (Fig. 1) might be ascribed to a back-reaction contribution (benzofuran + $H_2 \rightleftharpoons$ 2,3-dibenzofuran) or to somewhat stronger binding by 2,3-dibenzofuran than benzofuran. The first possibility is ruled out by the increased hydrogenation with *increasing* temperature (Fig. 1, curves A_3 (260°C) vs curve A_1 (220°C)). Thus, the relative binding strengths at 220–260°C on the catalyst appear to be given by

$$K_{2,3\text{-dibenzofuran}} \gtrsim K_{\text{benzofuran}} \gg K_{o\text{-ethylphenol}}.$$

Hydrodenitrogenation of nitrogen-containing compounds encounters an equilibrium limitation on the hydrogenation before removal of nitrogen atom from the ring (*8, 10, 14*). No such limitation for removal of oxygen from benzofuran was observed yet under the conditions employed in this investigation. However, saturation of an oxygen-containing ring was required before deoxygenation occurred. This agrees with the postulation of Landa *et al.* (*18*).

The present paper concerning benzofuran hydrodeoxygenation has demonstrated that considerable interactions exist among intermediates in the catalytic network of Fig. 11. A companion paper deals with HDO/HDS interactions involving benzofuran.

ACKNOWLEDGMENT

We are pleased to thank the National Science Foundation for support received to study multicomponent catalysts.

REFERENCES

1. Givens, E. N., and Venuto, P. B., *ACS Div. Petrol. Chem.*, Preprints 15, 4, A183 (1979).

2. Kilanowski, D. R., and Gates, B. C., *J. Catal.* **62,** 70 (1980).

3. Geneste, P., Amblard, P., Bonnet, M., and Graffin, P., *J. Catal.* **61,** 115 (1980).

4. Houalla, M., Nag, N. K., Sapre, A. V., Broderick, D. H., and Gates, B. C., *AIChE J* **24,** 1015 (1978).

5. Houalla, M., Broderick, D. H., Sapre, A. V., Nag, N. K., DeBeer, V. H. J., Gates, B. C., and Kwart, H., *J. Catal.* **61,** 523 (1980).

6. Singhal, G. H., Espiro, R. L., Sobel, J. E., and Huff, Jr., G. A., *J. Catal.* **67,** 457 (1981).

7. Singhal, G. H., Espino, R. L., and Sobel, J. E., *J. Catal.* **67,** 446 (1981).

8. Satterfield, C. N., and Cocchetto, J. F., *AIChE J.* **21,** 1107 (1975).

9. McIlvried, H. G., *Ind. Eng. Chem. Process Res. Dev.* **10,** 125 (1971).

10. Stern, E. W., *J. Catal.* **57,** 390 (1979).

11. Aboul Gheit, A. K., and Abidou, I. K., *J. Inst. Petrol.* **59,** (568), 188 (1973).

12. Shih, S. S., Katzer, J. R., Kwart, H., and Stiles, A. B., *Amer. Chem. Soc. Div. Petrol. Chem.* Preprints **22** (3), 919 (1977).

13. Rollman, L. D., *J. Catal.* **46,** 243 (1977).

14. Badilla, Ohlbaum, R., Pratt, K. C., and Trimm, D. L., *Fuel* **58,** 311 (1979).

15. Satterfield, C. N., Modell, M., and Mayer, J. F., *AIChE J.* **21,** 1100 (1975).

16. Bobyshev, V. I., Dyakova, M. K., and Lozovoi, A. V., *J. Appl. Chem.* (*USSR*) **13,** 942 (1940).

17. Hall, C. C., and Cawley, C. M., *J. Soc. Chem. Med.* **58,** 7 (1939).

18. Landa, S., Mrnkova, A., and Bertona, N., *Sci. Papers Inst. Chem. Tech. Prague* **D16,** 159 (1969).

19. Krishnamurthy, S., Panvelker, S., and Shah, Y. T., *AIChE J.* **27,** 994 (1981).

20. Odebunmi, E. O., "Heterogeneous Catalytic Hydrodeoxygenation of Cresols (Methyl Phenols) on Sulfided CoO-MoO_3/γ-Al_2O_3 Catalysts at High Temperature and Pressures," Ph.D. Dissertation, Princeton University (1981).

21. Shah, Y. T., "Reaction Engineering in Direct Coal Liquefaction." Addison–Wesley, Reading, Mass., 1981.

22. Whitehurst, D. D., Mitchell, T. O., and Farcasiu, M., "Coal Liquefaction. The Chemistry and Technology of Thermal Processes." Academic Press, New York, 1980.